

The beryllium abundance in the very metal-poor halo star G 64–12 from VLT/UVES observations[★]

F. Primas^{1,★★}, M. Asplund², P. E. Nissen³, and V. Hill¹

¹ European Southern Observatory, Karl-Schwarzschild Str. 2, D-85748 Garching b. München, fprimas@eso.org, vhill@eso.org

² Uppsala Astronomical Observatory, Box 515, SE-751 20 Uppsala, Sweden, martin@astro.uu.se

³ Institute of Physics and Astronomy, Aarhus University, Denmark, pen@ifa.au.dk

Received ; Accepted

Abstract. We report on a new spectroscopic analysis of the very metal deficient star G 64–12 ($[\text{Fe}/\text{H}]=-3.3$), aimed at determining, for the first time, its beryllium content. The spectra were observed during the Science Verification of UVES, the ESO VLT Ultraviolet and Visible Echelle Spectrograph. The high resolution ($\sim 48\,000$) and high S/N (~ 130 per pixel) achieved at the wavelengths of the Be II resonance doublet allowed an accurate determination of its abundance: $\log N(\text{Be}/\text{H}) = -13.10 \pm 0.15$ dex. The Be abundance is significantly higher than expected from previous measurements of Be in stars of similar metallicity (3D and NLTE corrections acting to make a slightly higher value than an LTE analysis). When compared to iron, the high $[\text{Be}/\text{Fe}]$ ratio thus found may suggest a flattening in the beryllium evolutionary trend at the lowest metallicity end or the presence of dispersion at early epochs of galactic evolution.

Key words: Stars: Population II, abundances, atmospheres — Galaxy: halo — Instrumentation: spectrographs

1. Introduction

The knowledge of lithium, beryllium, and boron in stars play a major role in our understanding of Big Bang nucleosynthesis, cosmic-ray physics, and stellar interiors. Lithium (together with D and He) is a key element to probe the Big Bang nucleosynthesis scenario, because most of ${}^7\text{Li}$ is primordially produced. On the contrary, ${}^6\text{Li}$, ${}^9\text{Be}$, ${}^{10,11}\text{B}$ (with a possible contribution to ${}^{11}\text{B}$ from ν -spallation in supernovae being still under debate) were

suggested to originate primarily from spallation reactions in the interstellar medium (ISM) between cosmic-ray (CR) α -particles and protons and heavy nuclei like carbon, oxygen, and nitrogen (Reeves et al. 1970). The production rate of any of these three light elements is then proportional to the product of the abundance of CNO (proportional to the number of supernovae, N_{SN}) and the CR flux (assumed to be proportional to the supernovae rate). A slope of two in the logarithmic plane ${}^6\text{Li}, {}^9\text{Be}, {}^{10}\text{B}$ vs O is thus expected. If $[\text{O}/\text{Fe}]$ in metal-poor halo stars is constant, then this same slope holds vs Fe as well.

On these premises, the picture emerging from the first systematic analyses of Be and B in stars of the Galactic halo and disk from high resolution data clearly challenged this scenario: both elements scale almost *linearly*, and not *quadratically* with metallicity from the early Galactic epochs up to now (e.g. Molaro et al. 1997, Boesgaard et al. 1999b for Be; Duncan et al. 1997, Primas et al. 1999 for B). Such finding has been interpreted as an indication for a primary (instead of secondary) origin of Be and B, that in turn may imply the need for a production mechanism independent of the metallicity in the ISM. Although the most recent theoretical scenarios (which seem to converge towards the proximity of supernovae as one of the most likely and efficient sites for Be and B production) are able to reproduce the observed abundance levels and trends, new observational inputs are still in high demand in order to further constrain the models. The evolution/behavior of Be at the lowest metallicities, the presence and magnitude of scatter (if any), the presence and location of a possible change of slope along the trend, and a successful solution of the oxygen dilemma (high or flat) in the Galactic halo are some of the still missing inputs.

With this Letter, we aim at adding a new tile to the field of light elements evolution, presenting the first beryllium detection in a star characterized by a metallicity well below one thousandth solar ($[\text{Fe}/\text{H}]=-3.3$), the halo star G 64–12. Our newly determined $[\text{Be}/\text{Fe}]$ ratio will be compared to previous observational analyses in low metallicity stars and confronted with different theoretical suggestions.

Send offprint requests to: F. Primas

[★] Based on observations taken during the Science Verification of UVES at the VLT/Kueyen telescope, European Southern Observatory, Paranal, Chile

^{★★} Visiting Researcher (CNRS) at the Laboratoire d'Astrophysique - Observatoire de Midi-Pyrénées, Toulouse, France

Table 1. Observations log for G 64–12

V	Date	Mode	λ_c nm	λ -coverage nm	Exp.Time min	S/N ^a
11.46	Feb. 12	Dic#1	346 (CD#1)	305–385	2×90	75,80
			580 (CD#3)	480–680	2×90	350,370
	Feb. 14	Dic#1	346 (CD#1)	305–385	2×80	65,70
			860 (CD#4)	665–1050	2×80	270,280

^a measured on each single spectrum, around 313 nm, 510 nm and 700 nm in the B346, R580, and R860 settings respectively

2. Observations and Data Reduction

A total of 6 hours integration time (cf Table 1 for more details) were devoted to G 64–12 ($V=11.45$ mag), during the Science Verification of UVES (February 10–18, 2000). The target was observed in Dichroic mode, and the six hours were splitted in four exposures of ~ 90 min each: two with the standard Dichroic #1 setting and two with a slightly modified Dichroic #1 setting. All the spectra were observed with a slit of $0.8''$, corresponding to nominal resolving powers of 48 000 in the blue and 55 000 in the red, later confirmed by the Thorium-Argon calibration frames. The spectra were reduced within the MIDAS UVES context. First, bias and inter-order background were subtracted from both science and flat-field frames, then the object was optimally extracted, divided by the flat-field (extracted with the same weighted profile as the star), λ -calibrated and the extracted orders merged. All the spectra were then registered for barycentric radial velocity shifts, co-added, and normalized. An independent check was performed using standard IRAF tasks for echelle spectra reduction, which produced the same final product. The S/N ratio achieved at the Be II resonance doublet on the final spectrum (cf Fig. 1) is 130 per pixel.

3. Stellar Parameters

Using the Infrared Flux Method, Alonso et al. (1996) derived $T_{\text{eff}} = 6470 \pm 90$ K for G 64–12. This is considerably higher than the value of $T_{\text{eff}} = 6220$ K determined by Ryan et al. (1999) from several colour indices using the “low” T_{eff} scale of Magain (1987). It should be noted, however, that Ryan et al. adopt a negligible low interstellar reddening of G 64–12, whereas the Strömgren $wvby$ - β photometry as given in their Table 1 suggests a reddening $E(b-y) = 0.023$ corresponding to $E(B-V) \simeq 0.03$. Correcting the colour indices for this reddening would increase the Ryan et al. temperature to about 6360 K. We conclude that the effective temperature of G 64–12 is quite uncertain; depending on the adopted reddening and the zero-point of the T_{eff} scale, one derives values between 6200 and 6500 K. However, fitting of the $H\alpha$ wings indicates a temperature closer to the higher end of the considered range of values ($T_{\text{eff}} \simeq 6400$ K).

The Hipparcos parallax of G 64–12 ($\pi = 1.88 \pm 2.90$ mas)

is too uncertain to be used to derive the surface gravity of the star. We note, however, that the position of G 64–12 in the $(b-y)_0 - c_0$ diagram (see Ryan et al. 1999, Fig. 3) is similar to that of HD 84937. Using the absolute magnitude calibration of Nissen & Schuster (1991), $M_V \simeq 3.6$ is derived for both stars. Hence, the gravity of G 64–12 must be close to that of HD 84937 ($\log g = 4.1$) as derived from its Hipparcos parallax (Nissen et al. 1997). Altogether, we estimate that the gravity of G 64–12 lies in the range $\log g = 3.9 - 4.3$.

The metallicity of G 64–12 was derived from equivalent widths of 22 Fe I lines in the spectral region 480 - 560 nm. The lines are weak ($2 < EW < 30$ mÅ), but the EW’s are very reliable due to the high S/N. Adopting gf -values from O’Brian et al. (1991) and using a 1D model atmosphere with $T_{\text{eff}} = 6400$, $[\text{Fe}/\text{H}] = -3.28 \pm 0.08$ dex is derived. Allowing for the possible range of T_{eff} (6300 - 6500 K), $[\text{Fe}/\text{H}] = -3.28 \pm 0.10$.

It is worth noticing that the same procedure applied to 5 Fe II lines yields a somewhat lower iron content $[\text{Fe}/\text{H}] = -3.42 \pm 0.10$. Though this would be in principle our preferred metallicity indicator (Fe II lines are much less sensitive to NLTE corrections), the gf -values of these lines are not very accurately known. Four out of five are listed in the compilation by Kroll & Kock (1987), and all five are found in the work by Moity (1983). Unfortunately, there is a systematic difference of ~ 0.20 dex between these two investigations (Moity’s values being lower). This has some consequences on the final iron abundance derived from these (few) lines, and certainly has a non-negligible effect on the derivation of $\log g$ from the ionization balance. We ran a few tests and reached the ionization balance for $\log g = 4.3$ if mean gf -values were adopted, and for $\log g = 4.1$ if Moity’s values were used. These results, together with the paucity of Fe II lines, made us decide to keep $\log g = 4.1 \pm 0.2$ as our final choice for the analysis.

4. Abundance Analysis Highlights

The analysis of the beryllium spectral region was performed via spectrum synthesis. For this purpose, we adopted a model atmosphere computed with $T_{\text{eff}} = 6400$ K, $\log g = 4.1$, and $[\text{Fe}/\text{H}] = -3.3$. Microturbulence was assumed to be 1.5 km s^{-1} .

The 1D spectrum synthesis analysis was carried out with

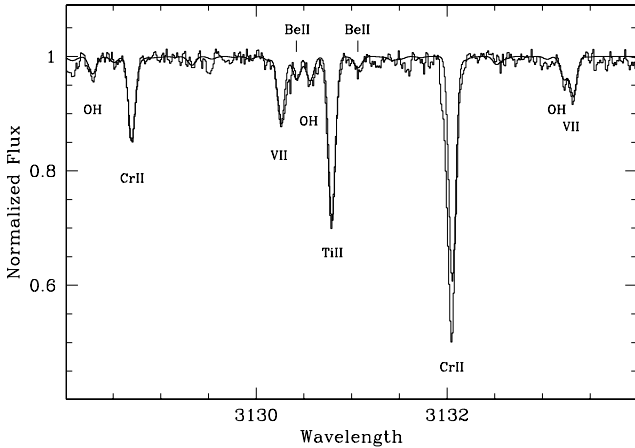


Fig. 1. Reduced and normalized observed spectrum of G 64–12 with overplotted our best-fit synthesis (thin line)

Kurucz model atmospheres and SYNTHE (Kurucz 1993). The model was convolved with a Gaussian function of $\text{FWHM} = 6.7 \text{ km s}^{-1}$ (which combines instrument, rotation and macroturbulence broadenings), and was computed with the α -elements enhanced by +0.4 dex and with the “approximate overshooting” option switched off. The solar abundances were taken from the compilation of Grevesse & Sauval (1998). The list of lines necessary to synthesize the near-UV spectral region is the one tested by Primas et al. (1997).

Additionally a time-dependent 3D hydrodynamical model atmosphere with parameters appropriate for G 64–12 has been constructed, with the same 3D, compressible, radiative-hydrodynamics code which has previously been successfully used for studies of solar and stellar convection (e.g. Stein & Nordlund 1998; Asplund et al. 1999, 2000). The equations of mass, momentum and energy coupled to the 3D radiative transfer equation (which includes the effects of line-blanketing) have been solved on a Eulerian mesh with $100 \times 100 \times 82$ zones covering $21 \times 21 \times 8.5 \text{ Mm}$. For the 3D LTE spectrum synthesis, a representative sequence of 1 hr stellar time with snapshots every 1 min was selected; the temporal average of T_{eff} for the sequence is $6460 \pm 27 \text{ K}$, i.e. very close to the value indicated by the IRFM method. It is noteworthy that no free parameters like mixing length parameters, micro- and macroturbulence enter the construction of 3D model atmospheres or spectral synthesis, as the time-dependent convective motions and inhomogeneities are self-consistently calculated. In order to quantify the systematic errors introduced when relying on 1D analyses, a strictly differential comparison of the 3D predictions have been carried out with a corresponding MARCS model (Gustafsson et al. 1975) with the same parameters and input data (Asplund et al. 1997).

4.1. On other Elemental Abundances

Because of the large spectral coverage (see Table 1), all the most commonly studied elements (α , iron-group, heavy) are accessible from the observed spectrum of G 64–12. Although the complete abundance analysis of G 64–12 is beyond the scope of this work, some of the elements most relevant to it deserve mentioning.

α -elements: we checked the abundance of magnesium and calcium in order to test how representative G 64–12 is of the population of the very metal-deficient stars. From the equivalent widths measured for two Mg Ib lines and four Ca I lines we derive $[\text{Mg}/\text{Fe}] = +0.43 \pm 0.03 \text{ dex}$ and $[\text{Ca}/\text{Fe}] = +0.48 \pm 0.07 \text{ dex}$, i.e. “normal” and in good agreement with what can be found in the literature.

Oxygen (from OH lines): the same spectral region where the Be II doublet falls is also very rich in OH molecular lines, which represent one of the few oxygen abundance indicators available to spectroscopists. Our 1D LTE spectrum synthesis analysis suggests $[\text{O}/\text{Fe}] = +1.1$, similarly to what found by Israelian et al. (1998) and Boesgaard et al. (1999a) using the same abundance indicator and for stars of comparable metallicity. Our finding is also in agreement with the recent oxygen determination made by Israelian et al. (2000) in the same star. However, due to severe systematic errors affecting the near-UV OH lines in metal-poor stars, we prefer not to adopt this value. We suspect that the oxygen abundance derived from the UV OH lines is in error, being affected by metallicity dependent 3D and/or NLTE effects (Asplund et al. 1999). A future analysis of Be in a larger sample of stars will deal with this issue (Primas et al., in preparation).

Lithium: the S/N ratio achieved around the Li I line at 670.8 nm is ≈ 300 . Our measurement of the Li I 670.8 nm equivalent width gives $\text{EW} = 22.2 \pm 0.5 \text{ m\AA}$, in agreement with the value published by Ryan et al. (1999, $\text{EW} = 21.2 \pm 1.1 \text{ m\AA}$). The lithium abundance derived is $A(\text{Li}) = 2.23 \pm 0.01 \text{ dex}$. The difference with Ryan et al. (1999) value ($A(\text{Li}) = 2.14 \pm 0.03 \text{ dex}$) can be explained by the difference in adopted temperatures.

5. The Beryllium Abundance and Its Uncertainty

The best-fit synthesis of the Be II doublet is achieved with $\log N(\text{Be}/\text{H}) = -13.20$ for the 313.0 nm line, and with $\log N(\text{Be}/\text{H}) = -13.10$ for the 313.1 nm line. Being both lines well resolved, equal weights were assigned. The beryllium abundance thus derived using Kurucz 1D LTE model atmosphere is $\log N(\text{Be}/\text{H}) = -13.15 \pm 0.15 \text{ dex}$, significantly higher than what is expected from extrapolating the previously observed trends to these low metallicities (under the assumption that the Be abundance keeps decreasing). The magnitude of the error-bar assigned to our measurement mainly comes from the dependence of the beryllium abundance on changes in the stellar parameters. In order of importance, we find that $\Delta \text{Be} = \pm 0.1 \text{ dex}$ for $\Delta \log g = \pm 0.2$, $\Delta \text{Be} = \pm 0.04 \text{ dex}$ for $\Delta T_{\text{eff}} = \pm 100 \text{ K}$,

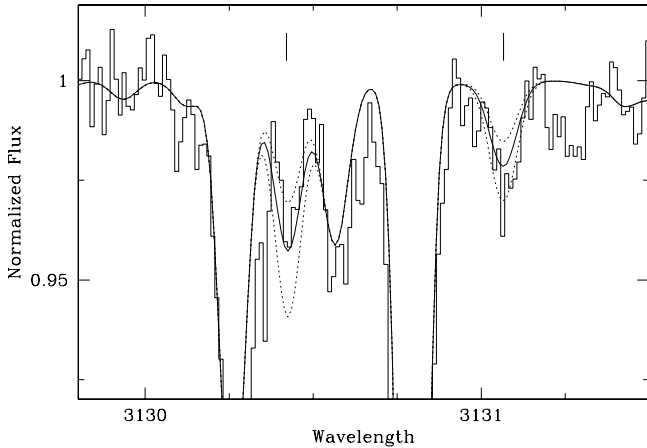


Fig. 2. An enlarged view of the Be II resonance doublet in G 64–12 (histogram), together with our best-fit synthesis (thin line). Overplotted are two syntheses computed with the beryllium abundance increased and reduced respectively by 0.15 dex (dotted lines)

and $\Delta\text{Be} = \pm 0.03$ dex for $\Delta[\text{Fe}/\text{H}] = \pm 0.1$ dex. To these values (to be summed in quadrature) one has to add the dependence of Be on the placement of the continuum. This uncertainty in such metal-poor star is estimated to be $\pm 1\%$ at most, implying a variation in Be of ± 0.05 dex. Fig. 2 shows an enlarged view of the Be doublet, with our 1D LTE best-fit synthesis, and two others computed with ± 0.15 dex variation in the Be content, which demonstrate our detection and measurement accuracy.

As expected, the predicted Be II line strengths with the 3D model atmosphere are quite similar to the 1D case, because the lines are formed in the deep atmospheric layers due to the lines being very weak and coming from the majority ionized species. Assuming LTE, the abundance correction derived by using 3D hydrodynamical model atmospheres is only 0.03 dex for Be II 313.1 in G 64–12, in the sense that the 1D abundance should be corrected upwards with 0.03 dex. It should be emphasized that the 1D–3D comparison has been done strictly differentially. The quoted differences are therefore estimates of the systematic errors due to the adopted model atmospheres one can expect when using a 1D analysis, regardless of whether Kurucz or MARCS model atmospheres have been used. Although the above-mentioned 3D effects are small, it should be borne in mind that these estimates assume LTE and there is no guarantee that the same will be true for NLTE. Recent improved 1D NLTE calculations appropriately done for G 64–12 with a very extended Be atom (71 levels compared to the 9 used by García López et al. 1995), find some small but significant NLTE effects. In terms of abundance, the NLTE abundance is 0.07 dex larger than the LTE result. In spite of the similarity with the LTE result, it should be noted that the line formation for the Be II lines is far from being in LTE, since the dominant

NLTE effects – over-ionization and over-excitation – have opposite influence on the line strength and thus the effects partly cancel. This may suggest that for some other stellar parameters the NLTE effects could be significantly larger. The details of the 1D NLTE calculations for Be II appropriate for a range of stellar parameters will be presented elsewhere (García Pérez et al., in preparation). It also remains to be investigated whether the steep temperature gradients and inhomogeneities in 3D model atmospheres may drive more pronounced departures from LTE, similar to recent calculations for Li and O (Asplund & Carlsson 2000; Asplund et al., in preparation).

6. The [Be/Fe] ratio

Our claim to have detected a significantly higher beryllium abundance in G 64–12 (compared to other low metallicity stars) can be more clearly seen when our new (1D LTE, for consistency with the rest of the sample) determination is plotted in a $\log N(\text{Be}/\text{H})$ vs. $[\text{Fe}/\text{H}]$ graph (cf Fig. 3a) together with carefully selected literature data of similar quality. All the data shown in Fig. 3 (both panels) had their Be abundances computed assuming a “high” T_{eff} scale, hence consistent with what we did.

Extrapolating the Boesgaard et al. (1999b) Be vs Fe relation at lower metallicities, our 1D LTE Be value is 0.6 dex higher (using their single line fit) or 0.8 dex higher (using their double line fit), regardless of the T_{eff} scale adopted. One may also compare G 64–12 to BD–04 °3208 (similar T_{eff} and $\log g$ but a factor of 10 higher metallicity, cf Boesgaard et al. 1999b) and note that their Be contents differ by a factor of 3 only (instead of the expected factor of 10, should Be and Fe grow at the same rate). From our measurements we also infer $[\text{Be}/\text{Fe}] = 2.15 \pm 0.19$, which is at least 0.5 dex off the average trend (Fig. 3b). Although we must say that G 64–12, together with the recent Be detection in LP 815–43 ($[\text{Fe}/\text{H}] = -2.95$, open triangle in Fig. 3; cf Primas et al. 2000), gives more weight to the hypothesis of a possible flattening of the Be trend at the lowest metallicities, at the moment, the interpretation of our new result is not straightforward. According to Vangioni-Flam et al. (1998), the finding of high Be abundances in stars with metallicity below $[\text{Fe}/\text{H}] = -3.0$ may favor shock acceleration in the gaseous phase of superbubbles produced by collective SNII explosions as the main mechanism of Be production. This, in turn, implies that the major role is played by the most massive stars only (say, with initial mass $M \geq 60M_{\odot}$).

According to the Parizot & Drury (1999) scenario, a double trend of Be vs O (and Fe) is expected depending on if the star formed inside a superbubble (hence with a high Be content due to the effect of collective SN explosions) or outside. In this case, we cannot exclude the possibility that G 64–12 may be representative of the “high” trend, whereas other previously studied very metal-deficient stars (like BD–13°3442, for instance,

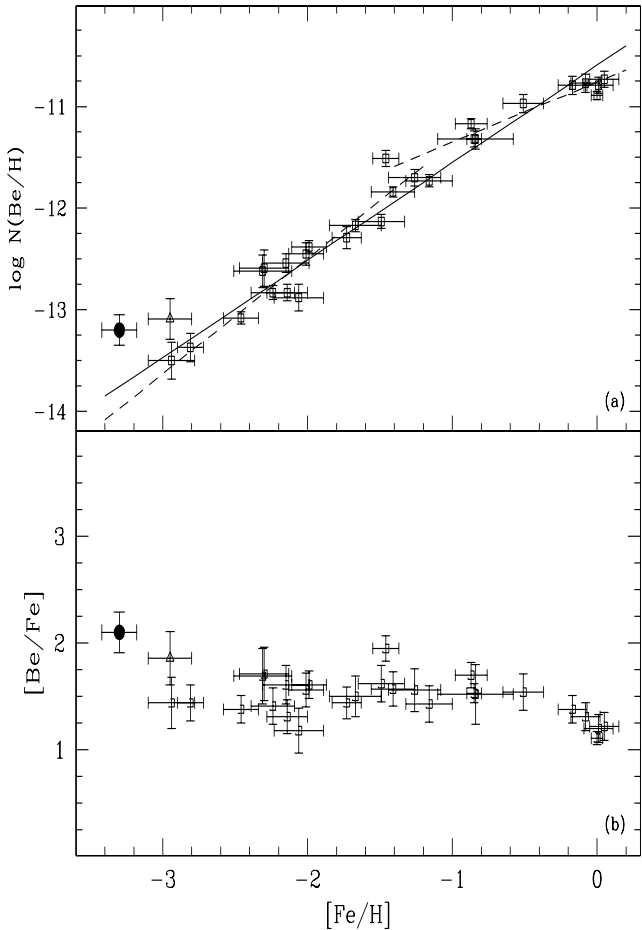


Fig. 3. Panel (a): $\log N(\text{Be}/\text{H})$ vs. $[\text{Fe}/\text{H}]$ for the highest quality data points currently available, with the Boesgaard et al. (1999b) least square fits overplotted (open squares from Boesgaard et al. (1999b), the open triangle is LP 815–43 from Primas et al. (2000), whereas the filled symbol represents this work – our 1D LTE value, for consistency with the rest of the data points); Panel (b): $[\text{Be}/\text{Fe}]$ vs $[\text{Fe}/\text{H}]$ for all the stars plotted in Panel (a) (same symbols have been adopted)

Boesgaard et al. 1999b) formed out of gas outside a superbubble. In order to test this hypothesis, new detections of beryllium in this challenging metallicity range are needed. One last possibility that should not be underestimated is the effect due to 3D and NLTE corrections. As previously stated, NLTE corrections have usually been assumed to be negligible, but they could be important for different combinations of stellar parameters. The future results of García Pérez et al. work will shed light on this issue.

7. Conclusions

We have presented a new analysis of the near-UV part of the spectrum of G 64–12 with the aim of studying its

beryllium content. The high quality of this UVES (Science Verification) spectrum has led to a clear detection of beryllium. This is the first measurement of Be in a star of such low metal content ($[\text{Fe}/\text{H}] = -3.3$). We have performed our analysis with 1D LTE model atmospheres, but introduced the novelty of correcting it for both 3D and non-LTE effects. Hence, our final 3D NLTE Be abundance is $\log N(\text{Be}/\text{H}) = -13.05 \pm 0.15$. We have shown that when compared in a consistent manner to previous high quality literature data, the Be abundance here detected is significantly higher than what expected. The strength of the OH molecular lines is comparable to what observed in other stars of similar metallicity, thus excluding the possibility that the high Be content measured in G 64–12 may be somehow related to an abnormally high O content. Furthermore, our measurement disagrees with the statement of a parallel (i.e. same rate) increase of Be and Fe, which, in turn, suggests a flattening or the presence of dispersion at given metallicity in the Be vs Fe trend during the early evolutionary phases of our Galaxy.

Acknowledgements. We thank the Science Operations (on Paranal) and the UVES Science Verification Teams for the efforts devoted to taking the observations and releasing the data to the ESO member states. A. García Pérez is thanked for making available to us her first results on new NLTE Be calculations, as well as E. Depagne for checking the $\text{H}\alpha$ fitting procedure. An anonymous referee is thanked for the quick report and the positive comments.

References

- Alonso A., Arribas S., Martínez-Roger C., 1996, *A&AS*, 117, 227
- Asplund M., Gustafsson B., Kiselman D., Eriksson K., 1997, *A&A* 318, 521
- Asplund M., Nordlund Å., Trampedach R., Stein R.F., 1999, *A&A* 346, L17
- Asplund M., Nordlund Å., Trampedach R., Allende Prieto C., Stein R.F., 2000, *A&A*, 359, 729
- Asplund M., Carlsson M., 2000, submitted to *A&A*
- Boesgaard A.M., King J.R., Deliyannis C.P., Vogt S.S., 1999a, *AJ*, 117, 492
- Boesgaard A.M., Deliyannis C.P., King J.R., Ryan S.G., Vogt S.S., Beers T.C., 1999b, *AJ*, 117, 1549
- Duncan D.K., Primas F., Rebull M.L., Boesgaard A.M., Deliyannis C.P., Hobbs L.M., King J.R., Ryan S.G., 1997, *ApJ*, 488, 338
- García López R.J., Rebolo R., Pérez de Taoro M.R., 1995, *A&A*, 302, 184
- Grevesse N., Sauval A.J., 1998, in: *Solar composition and its evolution – from core to corona*, Frölich C., Huber M.C.E., Solanki S.K., von Steiger R. (eds). Kluwer, Dordrecht, p. 161
- Gustafsson B., Bell R.A., Eriksson K., Nordlund Å., 1975, *ApJ* 42, 407
- Israelian G., García López R.J., Rebolo R., 1998, *ApJ*, 507, 805
- Israelian G., Rebolo R., García López R.J., Bonifacio P., Molero P., Basri G., Shchukina N., 2000, submitted to *ApJ*

- Kroll S., Kock M., 1987, A&AS, 67, 225
Kurucz R.L., 1993, CD-ROM # 1,13,18
Magain P. 1987, A&A 181, 323
Moity J., 1983, A&AS, 53, 37
Molaro P., Bonifacio P., Castelli F., Pasquini L., 1997, A&A, 319, 593
Nissen P.E., Schuster W.J., 1991, A&A 251, 457
Nissen P.E., Høg E., Schuster W.J., 1997, in Proc. ESA *Hipparcos* Symp., ESA SP-402, 225
O'Brian T.R., Wickliffe M.E., Lawler J.E., Whaling W., Brault J.W., 1991, J. Opt. Soc. Am. B. 8, 1185
Parizot E., Drury L., 2000, A&A, 356L, 66
Primas F., Duncan D.K., Pinsonneault M.H., Deliyannis C. P., Thorburn J. A., 1997, ApJ, 480, 784
Primas F., Duncan D.K., Peterson R.C., Thorburn J.A., 1999, A&A, 343, 545
Primas F., Molaro P., Bonifacio P., Hill V., 2000, A&A, in press
Ryan S.G., Norris J.E., Beers T.C., 1999, ApJ, 523, 654
Stein R.F., Nordlund Å., 1998, ApJ 499, 914
Reeves H., Fowler W.A., Hoyle F., 1970, Nature, 226, 727
Vangioni-Flam E., Ramaty R., Olive K.A., Cassé M., 1998, A&A, 337, 714